Chinese Journal of Polymer Science Vol. 33, No. 9, (2015), 1245–1259

Chinese Journal of Polymer Science
© Chinese Chemical Society
Institute of Chemistry, CAS
Springer-Verlag Berlin Heidelberg 2015

Synthesis and Liquid Crystalline Behavior of Side Chain Liquid Crystalline Polymers Containing Triphenylene Discotic Mesogens with Different Length Flexible Spacers*

Jian-feng Ban, Sheng Chen** and Hai-liang Zhang**

Key Laboratory of Polymeric Materials and Application Technology of Hunan Province, Key Laboratory of Advanced Functional Polymer Materials of Colleges and Universities of Hunan Province, College of Chemistry, Xiangtan University, Xiangtan 411105, China

Abstract A series of side chain liquid crystalline polymers (SCLCPs) containing triphenylene (Tp) units in the side chains, denoted as PMTS (without spacer) and PMT*n*S (*n* = 2, 3, 4, 6, which is the number of the methylene units between the main chain and Tp moieties in the side chains), with different lengths of spacers were synthesized through conventional free radical polymerization. The chemical structures of the monomers were confirmed by $^{1}H/^{13}C$-NMR, and the phase behaviors were examined by differential scanning calorimetry (DSC), polarized optical microscopy (POM) and wide-angle X-ray diffraction (1D and 2D WAXD). The molecular characterization of the polymers was performed with ^{1}H-NMR, gel permeation chromatography (GPC) and thermogravimetric analysis (TGA). The phase behaviors of the polymers have been investigated by a combination of techniques including DSC, POM, 1D and 2D WAXD. The results showed that the length of spacer has significant effects on the LC phase behavior of polymers. For PMTS and PMT2S, they displayed the columnar phase developed by the Tp moieties and the main chain as a whole due to the strong coupling effect of the Tp moieties and the main chain. For the PMT3S, PMT4S and PMT6S, they formed the symmetry hexagonal columnar (Φ_H) phase owing to the decoupling effect. All of these indicated that the "decoupling effect" or "coupling effect" depended on the length of spacers, leading to the different LC phase formation mechanism.

Keywords: Liquid crystalline polymer; Triphenylene; Flexible spacer; Phase behavior; Columnar phase.

Electronic Supplementary Material Supplementary material is available in the online version of this article at http://dx.doi.org/10.1007/s10118-015-1672-5.

INTRODUCTION

A great many side chain liquid crystalline polymers (SCLCPs) with differing structures have been reported in the literature because they show considerable application potential, but also they provide a demanding challenge to our fundamental understanding of the molecular factors that promote self-assembly in condensed systems[1–11].

SCLCPs contain four distinct structural components: the polymer backbone, the flexible spacer, the mesogenic group and the terminal substituent[12, 13]. For mesogenic groups, the discotic liquid crystals (DLCs) group has attracted great attention due to the capability of self-assembling into well different ordered structures because of the π-π stacking of the planar aromatic cores, which can be applied in many areas, such as optical

* This work was financially supported by the National Natural Science Foundation of China (No. 51373148) and the Innovation Platform Open Foundation of University of Hunan Province (No. CX2013B265).
** Corresponding authors: Sheng Chen (陈盛), E-mail: huaxuechensheng@163.com
Hai-liang Zhang (张海良), E-mail: zhl1965@xtu.edu.cn
Received January 21, 2015; Revised March 14, 2015; Accepted March 17, 2015
doi: 10.1007/s10118-015-1672-5

compensation films, one-dimensional conductors, anisotropic photoconductors and photovoltaic solar cells[14–20]. Since the first discovery of DLCs by Chandrasekhar *et al*. in 1977[21], many efforts have been devoted to the molecular modification of triphenylene (Tp) DLCs because of the easy synthesis, thermally and chemically stable and also varieties of mesophases[22, 23]. Therefore, the phase behavior and phase structure of the SCLCPs with the different Tp mesogenic groups and with different polymer backbones have been explored[24–27]. For example, several poly(methyl)acrylates and polysiloxanes containing Tp moieties in the side chains can form stable columnar phases[28–36]. Two series of Tp-containing polyacetylenes with different peripheral chain lengths[34] and with different flexible spacers[36] show a typical hexagonal (Φ_H) phase. A series of mesogen-jacketed liquid crystalline polymers (MJLCPs) containing two Tp units with different lengths of the methylene units between the terephthalate core and Tp moieties in the side chains can exhibit a variety of LC phases with variation of temperature[37, 38].

For the flexible spacer, much of the work focused on the nature and length of the spacer since the flexible spacer concept was established by Finkelmann *et al*[39, 40]. The role of the flexible spacer was considered necessary to decouple the interaction between backbone and mesogenic groups in the side chains. And the spacer length in SCLCPs can predominantly determine the mesophase types and properties of the polymers[41, 42]. For example, a series of dedronized polyacetylenes with short spacers were synthesized by Percec's group[43–45], the results show that the column shaped polymers can self-organize to form hexagonal or tetragonal columnar lattices. Imrie *et al*. have systematically studied the influence of flexible spacer length on the self-organization of the poly[ω-(4'-methoxybiphenyl-4-yloxy)alkyl methacrylatels and poly[ω-(4'-cyanobiphenyl-4-yloxy)alkyl methacrylatels[46, 47]. Our group has studied the phase behaviors of two series of side chain liquid crystalline poly(methyl)acrylates, containing triphenylene (Tp) units in the side chains (PMTS) with different molecular weights (M_n)[48]. The PMTS with no flexible spacer was amorphous when the M_n was lower than a critical M_n of approximately 2.03×10^4 g/mol. With M_n higher than this critical value, the PMTS displayed a columnar phase (Φ_R), while the phase structure of PMT6S (with six flexible spacers) were independent of M_n and the polymer displayed a symmetry hexaognal columnar phase Φ_H. In addition, our group has studied the phase behavior of the mesogen-jacketed liquid crystalline polymer (MJLCP) containing two triphenylene (Tp) units in the side chains (PBTCS)[49]. The results indicated that PBTCS got a relatively high glass transition temperature and formed a higher symmetry hexagonal columnar phase (Φ_H) due to the strong coupling effect between the Tp moieties and the MJLCP main chain.

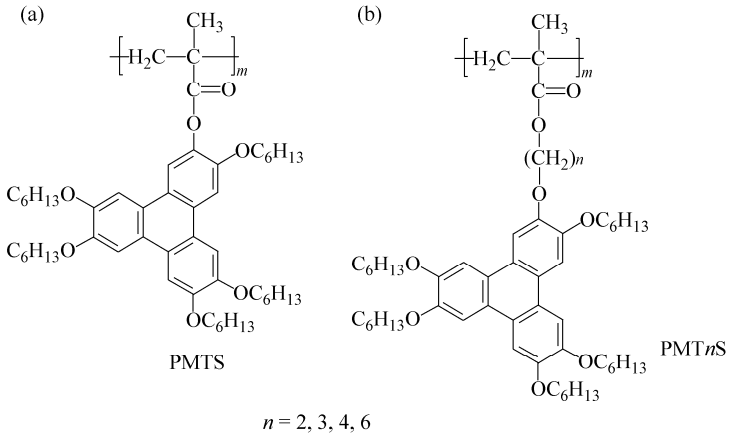


Chart 1 Chemical structure of PMTS (a) and PMT*n*S (b)

In this study, in order to systematically understand the influence of the spacer length on the phase structures and transitions of the SCLCPs containing triphenylene (Tp) units in the side chains, we have synthesized a series of Tp DLCs side chain liquid crystalline polymers with different flexible spacers *via* conventional free radical polymerization. The chemical structures of the polymers, poly{[3,6,7,10,11-pentakis(hexyloxy)-2-

oxytriphenylene] methacrylate} (PMTS with no flexible spacer) and poly{*n*-[3,6,7,10,11-pentakis(hexyloxy)-2-oxytriphenylene] methacrylate} (PMT*n*S, n = 2, 3, 4, 6), are shown in Chart 1. The results showed that they presented the absolutely different phase structures. Due to the strong coupling effect between the Tp moieties and the main chain, PMTS adopt a columnar shaped structure and self-organized into rectangular phases Φ_R. Similar to PMTS, PMT2S with the short spacer formed Φ_N phases developed by the Tp moieties and the main chain as a whole. For the polymers with $n \geq 3$ methylene flexible spacers presented a higher symmetry phase Φ_H owing to the decoupling and self-organization of the Tp moieties. All of these indicated the spacer affected the mechanism of LC phase structure formation in SCLCPs. To the best of our knowledge, this is the first time integrated report of SCLCPs polymers containing Tp mesogens with different length flexible spacers, which exhibiting fascinating ordered structures, and it can guide the design of ordered functional SCLCPs bearing Tp discotic mesogens.

EXPERIMENTAL

Materials

Anhydrous tetrahydrofuran (THF) was distilled from sodium benzophenone ketyl under argon and used immediately. Triethylamine (TEA) and dichloromethane (CH_2Cl_2) were dried over magnesium sulfate anhydrous. 2,2-Azobisisobutyronitrile (AIBN) was freshly recrystallized from methanol. Chlorobenzene (Acros 99%) was purified by washing with concentrated sulfuric acid to remove residual thiophenes, followed by twice washing, first with 5% sodium carbonate solution, and then with water before it was dried with anhydrous calcium chloride and distilled. All other reagents and solvents were used as received without further purification.

Instruments and Measurements

All NMR measurements were performed on a Bruker ARX400 MHz spectrometer using $CDCl_3$ as solvent, tetramethylsilane (TMS) as the internal standard at ambient temperature. The chemical shifts were reported on the ppm scale.

The apparent number average molecular weight (M_n) and polydispersity index (PDI = M_w/M_n) were measured on a GPC (WATERS 1515) instrument with a set of HT3, HT4 and HT5. The μ-styragel columns used THF as an eluent and the flow rate was 1.0 mL·min^{-1} at 38 °C. The GPC data were calibrated with polystyrene standards.

TGA was performed on a TA SDT 2960 instrument at a heating rate of 20 K·min^{-1} in nitrogen atmosphere.

DSC traces of the polymer were obtained using a TA Q10 DSC instrument. The temperature and heat flow were calibrated using standard materials (indium and zinc) at a cooling and heating rates of 10 K·min^{-1}. The sample with a typical mass of about 5 mg was encapsulated in sealed aluminum pans.

LC texture of the polymer was examined under POM (Leica DM-LM-P) equipped with a Mettler Toledo hot stage (FP82HT).

One-dimensional wide-angle X-ray diffraction (1D WAXD) experiments were performed on a BRUKER AXS D8 Advance diffractometer with a 40 kV FL tubes as the X-ray source (Cu Kα) and the LYNXEYE_XE detector. Background scattering was recorded and subtracted from the sample patterns. The heating and cooling rates in the 1D WAXD experiments were 10 K·min^{-1}.

Two-dimensional wide-angle X-ray diffraction (2D WAXD) was carried out using a BRUKER AXS D8 Discover diffractometer with a 40 kV FL tubes as the X-ray source (Cu Kα) and a VANTEC 500 detector. The point-focused X-ray beam was aligned either perpendicular or parallel to the mechanical shearing direction. For both the 1D and 2D WAXD experiments, the background scattering was recorded and subtracted from the sample patterns.

Synthesis of Monomers

The chemical structures and synthetic procedures of the monomers were shown in Scheme 1. The chemical structures of the monomers were confirmed by $^1H/^{13}C$-NMR. 2-Hydroxyl-3,6,7,10,11-pentakis (hexyloxy) triphenylene (PHT)[45, 46], the monomers [3,6,7,10,11-pentakis (hexyloxy)-2-oxytriphenylene] methacrylate (MTS) and 6-[3,6,7,10,11-pentakis (hexyloxy)-2-oxytriphenylene] hexyl methacrylate (MT6S) were easy to

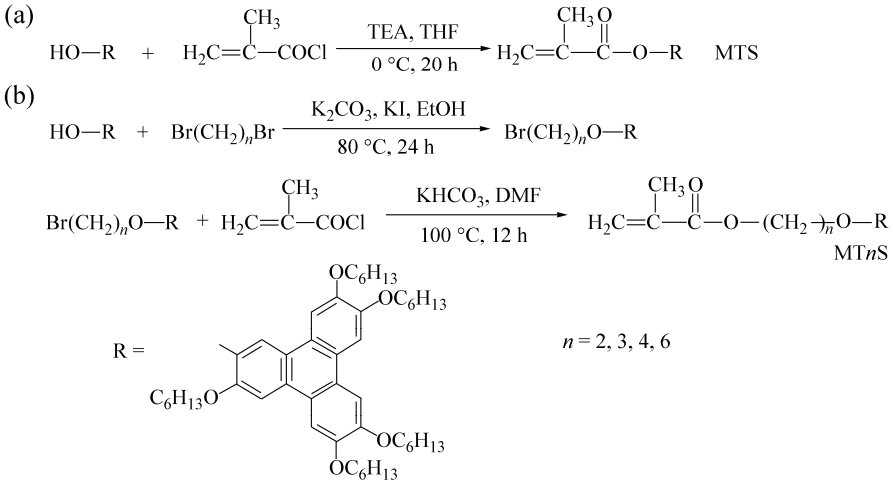
obtain according to our previous work[45].

According to literature[50], MT*n*S (*n* = 2, 3, 4) were easy to synthesize and obtain according to our work. The characterization data of the MT*n*S (*n* = 2, 3, 4) were as follows:

MT2S, ^{1}H-NMR (δ, CDC1$_3$): 7.99 (d 1H, Ar-H), 7.89–7.82 (a 1H, Ar-H, b 1H, Ar-H, c 1H, Ar-H, e 1H, Ar-H, f 1H, Ar-H), 6.19 (o 1H, =CH$_2$), 5.59 (n 1H, =CH$_2$), 4.66–4.48 (g 14H, −OCH$_2$−), 2.00–1.92 (m 3H, =C−CH$_3$), 1.62–1.48 (k 10H, −CH$_2$−, h 10H, −CH$_2$−, i 10H, −CH$_2$−), 1.44–1.33 (j 10H, −CH$_2$−), 0.99–0.90 (l 15H, −CH$_3$). ^{13}C-NMR (δ, CDC1$_3$): 167.30 (−C=O); 147.20 (C$_6$H$_5$−O); 135.45 (=C−); 127.02, 124.71, 121.01, 119.20, 106.32 (C$_6$H$_5$); 69.02, 68.74, 64.69 (−OCH$_2$−); 31.84, 29.89, 25.48, 22.77 (−CH$_2$−); 18.10, 14.11 (−CH$_3$).

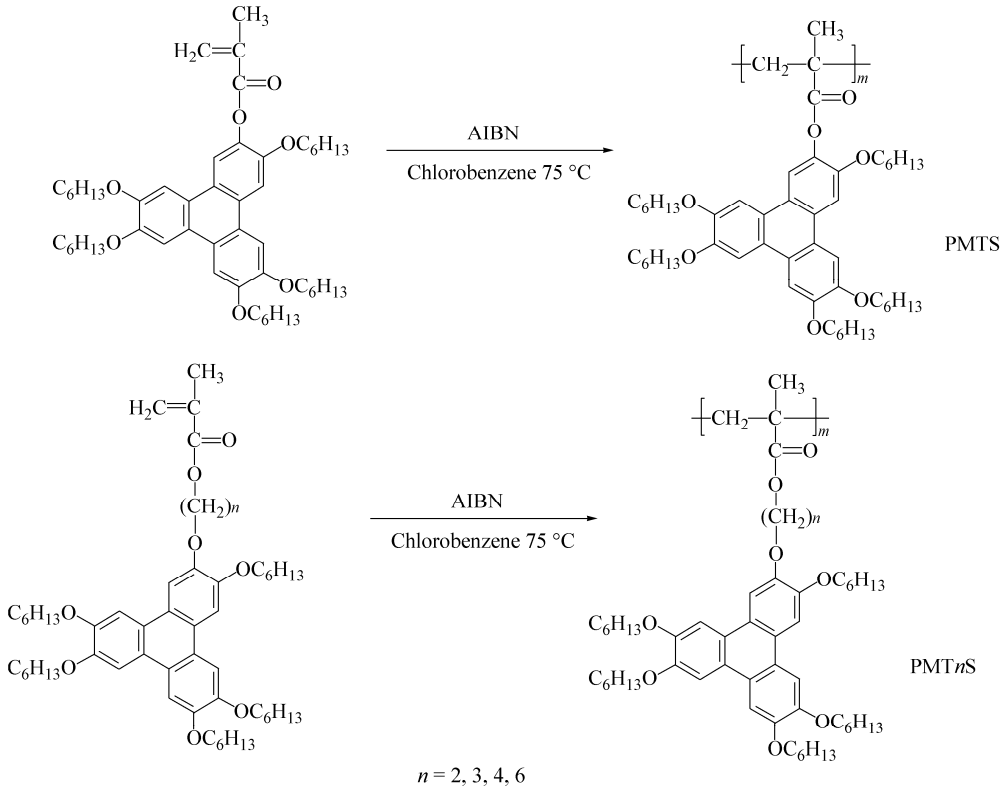
MT3S, ^{1}H-NMR (δ, CDC1$_3$): 7.98–7.71 (a 1H, Ar-H, b 1H, Ar-H, c 1H, Ar-H, d 6H, Ar-H, e 1H, Ar-H, f 1H, Ar-H), 6.18 (o 1H, =CH$_2$), 5.64 (n 1H, =CH$_2$), 4.66–4.21 (g 14H, −OCH$_2$−), 1.98–1.90 (m 3H, =C−CH$_3$), 1.65–1.32 (h 12H, −CH$_2$−, i 10H, −CH$_2$−, j 10H, −CH$_2$−, k 10H, −CH$_2$−), 0.91–0.78 (l 15H,−CH$_3$). ^{13}C-NMR (δ, CDC1$_3$): 167.21 (−C=O); 146.80 (C$_6$H$_5$−O); 136.05 (=C−); 126.11, 123.72, 122.66, 118.39, 106.82 (C$_6$H$_5$); 69.12, 65.25, 62.65 (−OCH$_2$−); 32.02, 29.59, 28.52, 25.71, 22.84 (−CH$_2$−); 18.30, 14.08 (−CH$_3$).

MT4S, ^{1}H-NMR (δ, CDC1$_3$): 7.99–7.73 (a 1H, Ar-H, b 1H, Ar-H, c 1H, Ar-H, d 6H, Ar-H, e 1H, Ar-H, f 1H, Ar-H), 6.20 (o, 1H, =CH$_2$), 5.61 (n, 1H, =CH$_2$), 4.68–4.20 (g 14H, −OCH$_2$−), 1.99–1.92 (m 3H, =C−CH$_3$), 1.66–1.34 (h 10H, −CH$_2$−, i 10H, −CH$_2$−, j 10H, −CH$_2$−, k 10H, −CH$_2$−), 0.90–0.78 (l 15H, −CH$_3$). ^{13}C-NMR (δ, CDC1$_3$): 167.44 (−C=O); 146.70 (C$_6$H$_5$−O); 136.72 (=C−); 126.15, 123.69, 122.08, 118.18, 106.66 (C$_6$H$_5$); 69.73, 68.75, 65.12 (−OCH$_2$−); 31.88, 29.50, 25.60, 25.44, 25.02, 22.77 (−CH$_2$−); 18.07, 14.11 (−CH$_3$).



Scheme 1 Synthetic route of the monomers

As shown in Scheme 2, the polymer was synthesized by conventional solution free-radical polymerization. Take PMTS as an example, the detailed procedure was carried out as follows: 0.2 g (0.25 mmol) of MTS, 100 μL of chlorobenzene solution of 0.01 mmol AIBN, 2 mL of chlorobenzene, and a magnetic stir bar were added into a polymerization tube, the tube was purged with nitrogen and subjected to three freeze thaw cycles to remove any dissolved oxygen and sealed off under vacuum. Polymerization was performed at 75 °C for 12 h. Subsequently, the polymerization was stopped by dipping the tube in ice water. Then the reaction mixture was diluted with 10 mL of THF. The resultant polymer was precipitated and washed with methanol. To eliminate the unreacted monomers completely, the purification was repeated for three times, until no peak was observed at the elution time of monomer in gel permeation chromatography (GPC) measurement. The polymers followed by drying at 50 °C under vacuum for 24 h, the target polymers of PMTS and PMT*n*S were obtained.



Scheme 2 Synthetic route of the polymers

RESULTS AND DISCUSSION

Synthesis and Characterization of Monomers and Polymers

All the monomers were easy to obtain *via* acyl chloride reaction. And the monomers could be easily polymerized *via* free radical polymerization. GPC analysis showed that all polymers were good polymerizability of the monomers. The molecular characterizations of the polymers are summarized in Table 1. The chemical structures of the monomers were confirmed by $^{1}H/^{13}C$-NMR. Take MTS (Fig. S1a), MT4S and MT6S (Fig. S1b) as the example. Figures 1(a) and 1(b) give the ^{1}H-NMR spectra ($CDCl_3$) of the monomer MT4S and polymer PMT6S, respectively. As shown in Fig. 1(b), the characteristic resonances of vinyl groups appearing at $\delta = 6.10$ and 5.53 completely disappear after polymerization, and the resonance peaks of PMT6S are rather broad and consistent with the expected polymer structure, indicating the successful polymerization as well.

Table 1. Molecular characteristics of the polymers

Sample	M_n [a] ($\times 10^4$)	PDI [a]	T_i [b] (°C)	T_g [c] (°C)	T_d [d] (°C)
PMTS	3.2	1.94	220	153	381
PMT2S	4.1	2.45	202	124	380
PMT3S	3.9	1.72	164	68	382
PMT4S	4.2	1.84	136	56	383
PMT6S	4.6	1.71	86	42	379

[a] Determined by GPC in THF using PS standards;

[b] Isotropization temperature evaluated by POM at a heating rate of 5 K·min^{-1};

[c] Evaluated by DSC during the second heating process at a rate of 10 K·min^{-1}, under nitrogen atmosphere;

[d] Temperature of 5% weight loss Evaluated by TGA under nitrogen atmosphere at a heating rate of 20 K·min^{-1}.

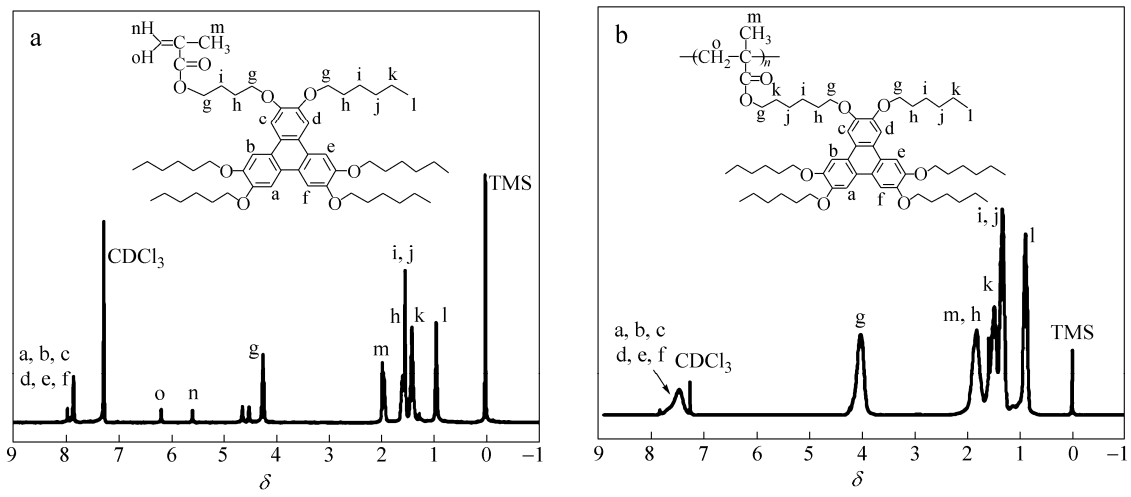


Fig. 1 ^{1}H-NMR spectra of monomers MT4S (a) and PMT6S (b) in $CDCl_3$

Mesomorphic Properties of the Monomers

The mesomorphic transitions of the monomers were investigated by differential scanning calorimetry (DSC), polarized optical microscopy (POM), and combined with onedimensional wide angle X-ray diffraction (1D WAXD). The results show that all the monomers exhibit enantiotropic liquid crystallinity. The DSC thermograms of the monomers are shown in Fig. 2, and the mesomorphic textures of MTS, MT4S and MT6S are depicted in Fig. 3 as examples. POM observation reveals that upon cooling from the isotropic liquid to 45 °C, the monomers show pseudo focal-conic fan textures, which is the typical texture of columnar phase[51–53]. The DSC thermogram recorded in the second heating cycle shows only a single transition peak. With the aid of POM, the peak was assigned to the transition from the columnar phase to the isotropic state because typical pseudo focal-conic fan texture is observed when the monomer is cooled to below this transition temperature.

Take MT4S as the example, when heating to 50 °C, the textures disappeared, indicating transition into isotropic state, which was consisted with the DSC results (Once the temperature reaches 155 °C (MTS), 87 °C (MT2S), 58 °C (MT3S), 50 °C (MT4S) and 49 °C (MT6S), respectively, the bright conformation disappeared, and the field of vision became dark, an isotropic state was observed). The mesomorphism is enantiotropic associated with Col-I transition is detected in the second heating scan. Although all the monomers form the same mesphase, the isotropization temperature (T_i) varies with the length of spacer. The T_i decreased from 155 °C for MTS to 49 °C for MT6S.

The phase transitions and structures of the monomers were further verfied on the 1D WAXD instrument. Figure 4 illustrates the 1D WAXD patterns at 125 °C for MTS, 75 °C for MT2S, 50 °C for MT3S, 45 °C for MT4S and 40 °C for MT6S, during the first cooling. As shown in Fig. 4, take MTS for example, only a strong peak at 4.75° with a *d*-spacing of 1.86 nm was detected in the low-angle region, while in the high-angle region, a weak amorphous halo at ~21° corresponding to the liquid-like order of the alkoxy tails and a strong peak at ~25° (seen the arrow in Fig. 4) with a *d*-spacing of 0.36 nm, which is an indicative of ordered stacking of the triphenylene cores with intermolecular π-π interaction were observed. The intensity of the peak corresponds to the π-π interaction between the triphenylene cores decreased with the spacer increased. The *d*-spacing was slightly decreased with the spacer increase, indicating the molecular plane of MT6S is nearly perpendicular to the formed column axis and that of MTS, MT2S, MT3S and MT4S will tilt a small angle.

Thermal and Liquid Crystalline Properties of the Polymers

The thermal and liquid crystalline properties of the polymers were investigated by TGA, DSC and POM. As shown in Table 1, the polymers exhibit excellent thermal stability, the temperatures at 5% weight loss of the samples under nitrogen were above 370 °C measured by TGA at a rate of 20 K·min^{-1}, which was much higher

than that of small molecule Tp DLCs. Thus, the incorporation of the Tp into the side chain of the polymethylacrylic acid structure has dramatically enhanced the resistance to thermolysis.

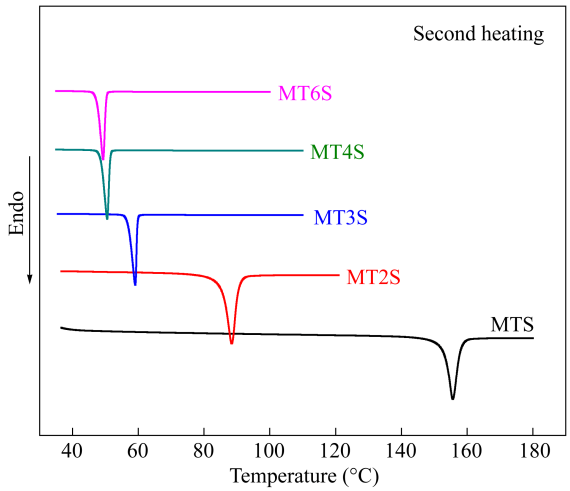


Fig. 2 DSC curves of monomers during the second heating scan at a rate of 10 K·min^{-1} under nitrogen atmosphere

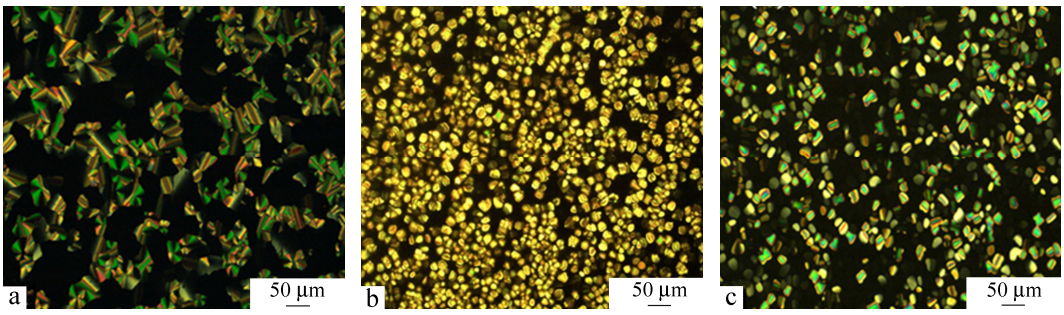


Fig. 3 POM images of the texture of MTS (a), MT4S (b) and MT6S (c)

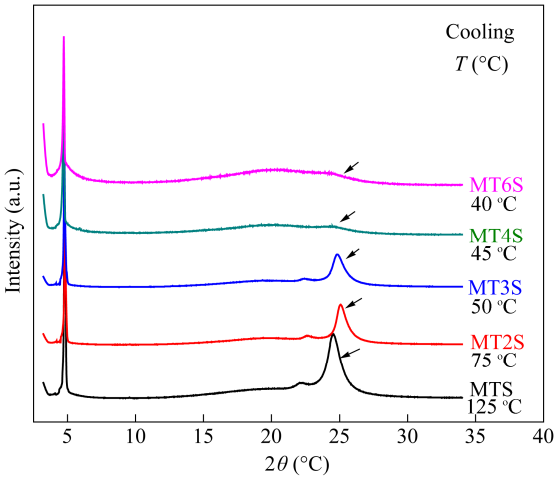


Fig. 4 1D WAXD patterns of monomers during the first cooling

The phase transition behaviors of the polymers were investigated by DSC. Figure 5 presents DSC curves of the polymers during the second heating cycle at a rate of 10 K·min^{-1} under nitrogen atmosphere after eliminating

the thermal history. The values of transition temperatures for all samples are listed in Table 1. As can be seen in Fig. 5(a), PMTS and PMT2S show only a glass-transition step but no endothermic peak correlating to a phase transition during the second heating scans. This phenomenon is similar to that of MJLCPs and the whole rigid columnar shaped polymethylacrylic acid molecule acted as the building block of the LC phase but not the side chain Tp mesogens only. For PMT3S, PMT4S and PMT6S as can be seen in Fig. 5(b), a glass-transition step and an endothermic peak were observed in all these samples. According to the literature[33] and the POM results, this endothermic peak attributed to transitions from LC phase to isotropic phase. As expected, the PMTS got a relatively higher T_g (153 °C). When n = 2, 3, 4, 6, the T_g of the polymers was 124 °C, 68 °C, 56 °C and 42 °C, respectively. Meantime, the transition temperatures (T_i) decreased from 220 °C to 86 °C with the increase of flexible spacer from no spacer to 6 methylene units.

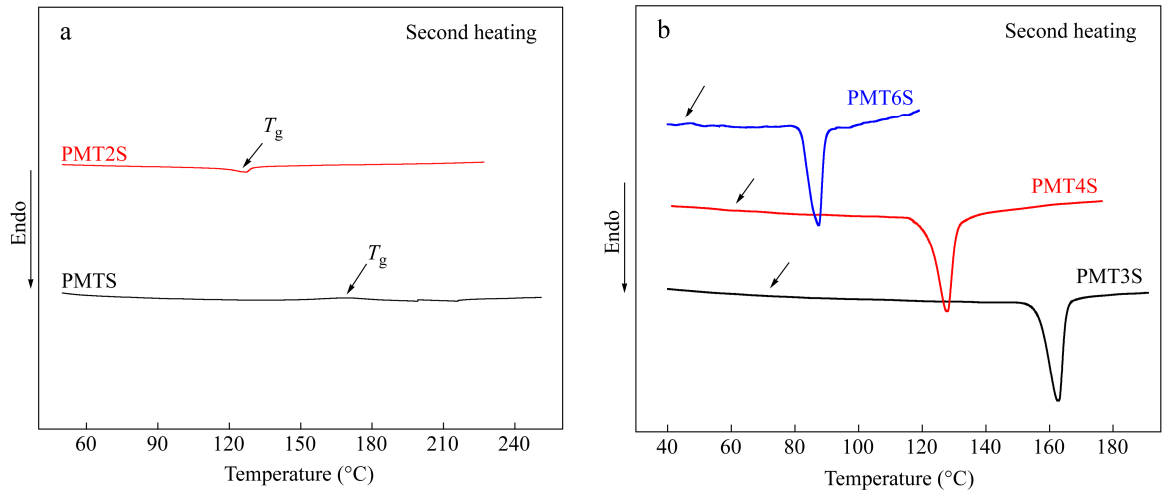


Fig. 5 DSC thermograms of polymers during the second heating at a rate of 10 K·min^{-1} under nitrogen atmosphere

Polarized optical microscopy (POM) experiments further confirmed the DSC results. To be consistent with the DSC result (the second heating), all samples were heated to the same high temperature as the DSC test and then slowly cooled to the room temperature. The POM results are shown in Fig. 6. As can be seen from it, the polymers formed the two different LC textures. For the PMTS and PMT2S, taking the PMTS as the example, PMTS formed colorful LC texture at the room temperature (as can be seen in Fig. 6a). With the heating procedure, the samples maintained zero birefringence until over 220 °C. During cooling from 220 °C, no LC textures were observed again in low temperature. This phenomenon was considered that as the flexible spacer was abolished, in order to minimize the torque arising from the rigid side chains of Tp DLCs, the backbone was compelled to stretch to a great extent. Thus the bulky side chain would be wrapped around the main chain and the whole rigid columnar shaped molecule of the PMTS acted as the building block of the LC phase but not the side chain Tp DLCs only. The sample for PMT2S (Fig. 6b) showed similar results to PMTS.

For the PMT3S, PMT4S and PMT6S, taking the PMT3S as the example, the observation of POM was shown in Fig. 6(c). With slow heating, PMT3S became soft and formed pseudo focal-conic fan textures, which was the typical texture of columnar phase. Once the temperature reached 164 °C, the LC texture disappeared and the field of vision became dark, indicating that PMT3S entered into the isotropic state, a corresponding exothermic peak appeared in DSC curve (Fig. 4b). When cooled to room temperature from 164 °C, LC textures were observed again, implying the forming of ordered structure was reversible. Therefore, it was considered that the phase transitions of PMT3S followed the sequence of columnar phase ↔ isotropic phase. The samples for PMT4S and PMT6S showed similar results to PMT3S. The transition temperatures from columnar phase to isotropic phase (measured by POM) are shown in Table 1. As can be seen (Fig. 7), T_i and T_g decreased with the increase of the spacer, which identified with the DCS result.

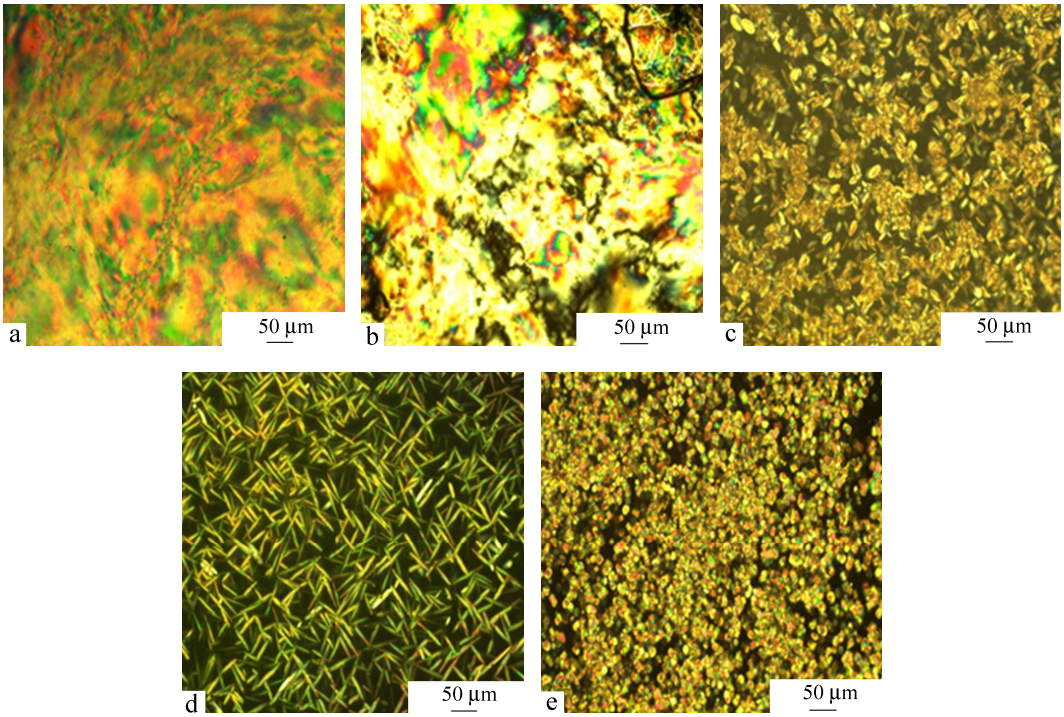


Fig. 6 Representative POM images of the texture of PMTS (a), PMT2S (b), PMT3S (c), PMT4S (d) and PMT6S (e)

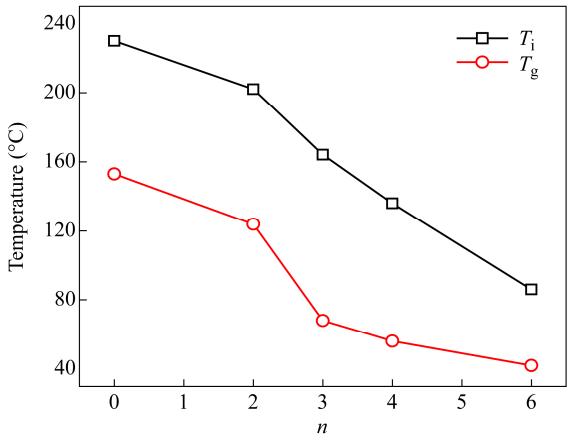


Fig. 7 The transition temperatures of PMTS and PMT*n*S

Phase Structure Identification of the Polymers

In order to study the mesomorphic structures of the polymers, temperature dependant 1D WAXD experiments were conducted. For 1D WAXD experiments about 50 mg of the polymer was added into an aluminum foil substrate. In order to be consistent with the DSC and POM results, the sample was heated to the same high temperature as in the DSC and POM tests, and then slowly cooled to the room temperature. The temperature was not higher than 300 °C during the experiments for the sample to avoid thermal degradation. 1D WAXD experiment results showed that the polymers exhibited difference phase structures, which was consistent with the POM result. 1D WAXD profiles of the polymers during the second heating processes are shown in Fig. 8, respectively.

Figure 8(a) shows the 1D WAXD powder patterns of PMTS during the second heating. The as-cast sample renders one peak in the low-angle region, indicating the existence of an ordered structure. In the wide-angle region, two amorphous peaks are found at 2θ values of ~20° ($d \approx 0.44$ nm) and ~24° ($d \approx 0.37$ nm). These two peaks in the wide-angle region represent the characteristic dimensions of the amorphous packing of the alkyl chains and the π-π stacking in a discotic LC column. However, the weak intensity of π-π stacking indicated that Tp moieties did not have good self-organizing into a well-ordered supramolecular LC column. After heating to higher temperatures, taking at 150 °C as an example, two peaks develop in the low-angle region, and the broad halo in the wide-angle region slightly shifts to lower angles due to thermal expansion. The corresponding *d*-spacing values of the two peaks in the low-angle region are 1.83 and 1.65 nm, which can be assigned as (100) and (010), diffractions of a rectangular structure with a = 1.83 nm, b = 1.65 nm, and γ = 90°, and this rectangular structure possesses only a 2D positional order, exhibiting features of a columnar phase, similar to many MJLCPs[54, 55]. Because of the possible rotation of the ester linkage, the whole side-chain length cannot be precisely estimated. However, depending on the relative position of Tp moieties in the side chain, the dimension of the whole side chain should be in the range of 2.3–4.6 nm. This range includes the sizes of the aforementioned 2D rectangular structure (a = 1.83 nm and b = 1.65 nm). Therefore, we speculated that PMTS forms a 2D rectangular columnar (Φ_R) phase developed by the bulky rigid side chains of Tp DLCs wrapping around the main chain.

The 1D WAXD profiles of PMT2S are similar to those of PMTS. To some extent, as shown in Fig. 8(b), two amorphous halos are found at 2θ values of ~18° ($d \approx 0.49$ nm) and ~22° ($d \approx 0.40$ nm), which represent the characteristic dimensions of the amorphous packing of the alkyl chains and the π-π stacking in a discotic LC column in the wide-angle region, suggesting that PMT2S exhibited the weak intensity of π-π stacking. On the other hand, the sample renders one peak in the low-angle region, 2θ = 5.12° ($d \approx 1.73$ nm), indicating the existence of an ordered structure. And this ordered structure can be identified as a Φ_N phase developed by the main chain and Tp as a whole. Generally, Tp DLCs tend to stack on one another to self-organize into a well-ordered supramolecular column because of the π-π stacking, lead to that many Tp derivatives including Tp-based side chain LC polymers form 2D Φ_H phases at ambient temperature[28–31, 56]. However, for our polymers, we speculate that, for PMTS with no flexible spacer, and for PMT2S with the short flexible spacer, the whole polymer behaves more like the individual MJLCPs, and the Tp moieties become more-or-less part of the side chains of the main chain because of the strong coupling effect of the Tp moieties and the main chain.

For PMT3S (Fig. 8c), PMT4S (Fig. 8d) and PMT6S (Fig. 8e), with the spacer increased, the molecular packing model was changed. Take PMT6S as an example, two diffractions peaks in the low-angle region at 2θ = 4.60° and 8.01° were detected at room temperature, the *d*-spacing derived from these two peaks were 1.92 and 1.10 nm, which have the typical ratio of the q values of $1:3^{1/2}$ and the two peaks can be assigned as (100) and (110) diffractions, demonstrating a long-range ordered hexagonal lattice with $a = b$ = 2.21 nm and γ = 120°. With the temperature increased, the two diffraction peaks in the low-angle region and the broad halo in the wide-angle region become weaken and the peak positions slightly shift to low-angle due to thermal expansion. Similar to PMTS and PMT2S, two amorphous halos at 2θ values of ~19° ($d \approx 0.46$ nm) and ~24° ($d \approx 0.37$ nm) were found in the wide-angle region. The same positions of the two peaks are found in the wide-angle region, because the two peaks belong to amorphous packing of the alkyl chains and π-π stacking of the Tp. From the 1D WAXD test results we found, the π-π stacking (2θ values of ~25°) were more intense with the spacer increase. This intensity difference suggests that longer flexible spacers between the main chain and Tp moieties in the side chains offer a stronger decoupling effect, which allows Tp moieties act more independently. As can be seen in Fig. 8(e), when n = 6, the intensity of π-π stacking was the highest, indicating that the ordered structure formed by Tp moieties in PMT6S was more ordered due to the long spacer decoupling effect. Meanwhile, as can be seen in Fig. 8(a) and Fig. 8(b), the intensity of π-π stacking of PMTS and PMT2S was lower compared to that of PMTnS (n = 3, 4, 6), owing to the strong coupling effect between the main chain and Tp moieties in the side chains.

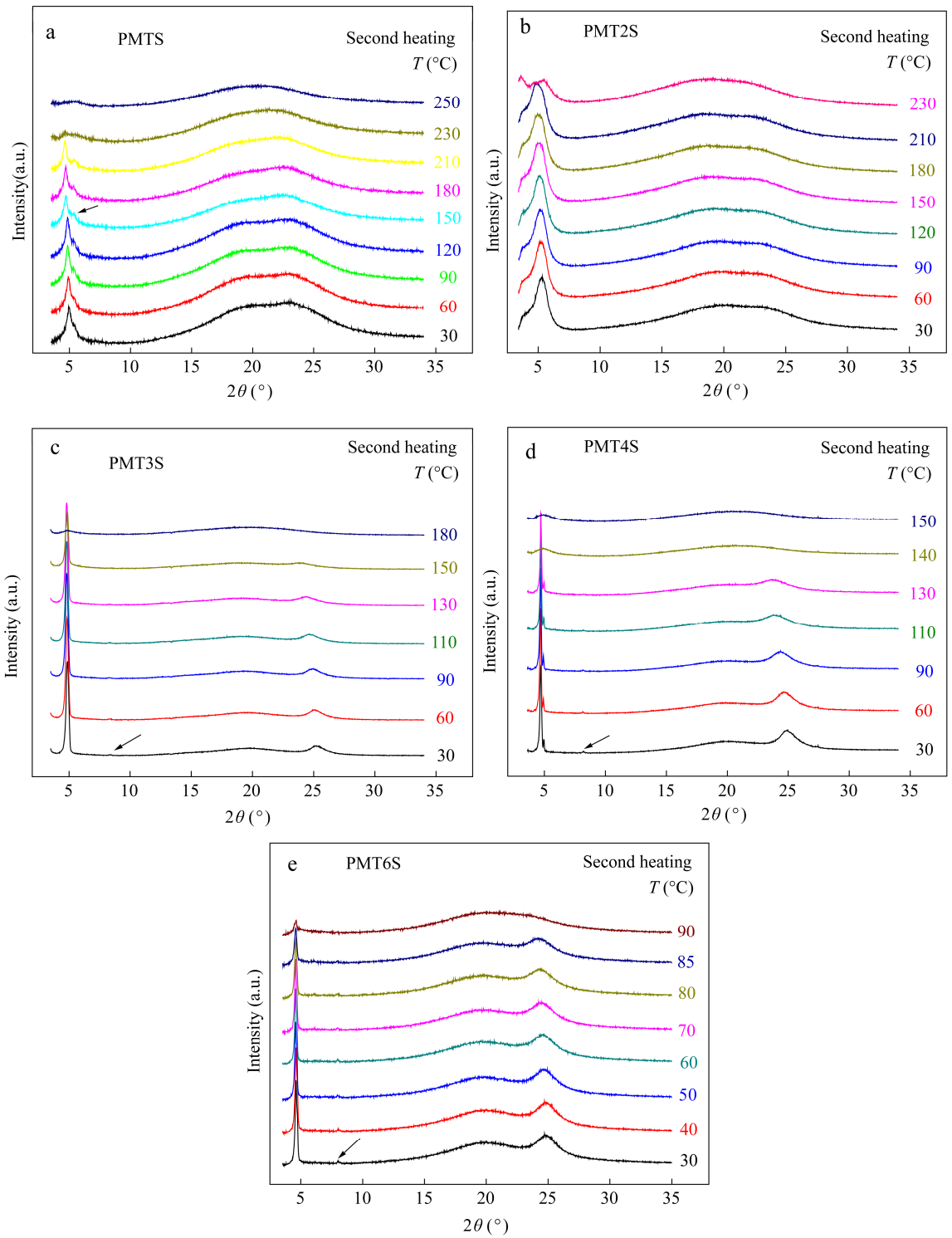


Fig. 8 1D WAXD patterns of the PMTS (a), PMT2S (b), PMT3S (c), PMT4S (d) and PMT6S (e) during the heating process of the as-cast film

The 1D WAXD patterns for PMT6S were used to calculate the diameter of the column, which is 2.21 nm comparable to the simulated length of the Tp moieties with all-trans conformation of C6 alkyl arms (~2.3 nm).

The larger a and b values in the 2D rectangular unit cell of PMT6S compared with PMT3S and PMT4S (Table 2 summarizes the values of d-spacing) are owing to the increased spacer length from three methylene units to six ones, Tp moieties in PMT6S act more independently, thus, the Tps self-organize into a well-ordered structure, the molecular plane of PMT6S is nearly perpendicular to the formed column axis. As can be seen in Fig. 9, the phase diagram of the polymers shows the change of Φ_R (PMTS) → Φ_N (PMT2S) → Φ_H (PMT3S, PMT4S and PMT6S) with the increasing of the flexible spacer.

Table 2. The 2θ d-spacing values and calculated length of the mesogenic units

Sample	2θ [a] (°)	d-spacing [a] (nm)	Calculated diameter of the column (nm)
PMTS	5.01	1.83	2.02
PMT2S	5.12	1.73	1.99
PMT3S	4.77	1.85	2.12
PMT4S	4.71	1.88	2.16
PMT6S	4.62	1.92	2.21

[a] Obtained from the one-dimensional WAXD experiments

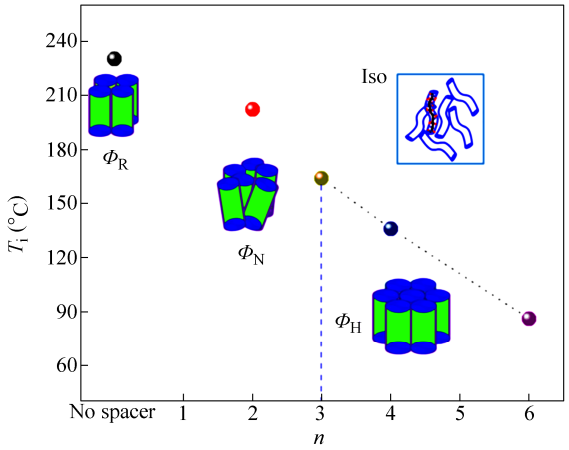


Fig. 9 The phase diagram of PMTS and PMTnS (n is the number of the alkyl spacer, n = 2, 3, 4, 6)

In order to further characterize the detailed mesomorphic structures of the polymers, 2D WAXD experiments were conducted. The 2D WAXD patterns at room temperature are shown in Fig. 10. All fiber samples were drawn with a pair of tweezers at temperatures above glass-transition temperature. In this figure, the X-ray beam is perpendicular to the shear direction that is along the meridian. For PMTS, as can be seen in Fig. 10(a), a pair of diffraction arcs with d-spacing values of 1.83 nm was located on the equator. This result further confirms the conjecture on the basis of 1D WAXD experiments that the diffraction with the d-spacing of 1.83 nm in the low-angle region is the d_{100} of the Φ_R phase. Similar to PMTS, for PMT2S (seen in Fig. 10b), PMT3S (seen in Fig. 10c), PMT4S (seen in Fig. 10d) and PMT6S (seen in Fig. 10e), a pair of diffraction arcs with d-spacing values (seen in Table 2) of 1.73 nm, 1.85 nm, 1.88 nm and 1.92 nm was located on the equator and the meridian, respectively. This result further confirms the conjecture on the basis of 1D WAXD experiments that the diffraction with the d-spacing in the low-angle region is the d_{100}.

To get a detailed investigation into the columns formed by the PMTS and PMTnS, the packing model of the columns and molecular dynamic simulation results of PMTS and PMTnS are shown in Fig. 11. From the whole tests, we found that PMTS and PMT2S exhibit a stabilized phase structure. For samples without or with short (n = 2) flexible spacer between the polymethylacrylic acid main chain and Tp moieties in the side chains the strong coupling effect overcomes the π-π interaction of Tp mesgeon. The simulated analysis of PMTS showed that the Tp side chain wrapped around the main chain to form a rectangular columnar shaped molecule with a = 1.83 nm, b = 1.65 nm, and γ = 90°, as shown in Fig. 11. In the columnar shaped molecule, the side chain Tp tilts an angle of ~30° off the main chain. Similar to PMTS, PMT2S showed that the Tp side chain wrapped around

the main chain, and form a columnar shaped molecule with r = 1.68 nm, and the side chain Tp tilts an angle of ~22° off the main chain. Increasing the length of the flexible spacer between main chain and Tp moieties in the side chains offers a stronger decoupling effect. Therefore, PMTnS (n = 3, 4, 6) act like small molecule of Tp DLCs with Φ phases (Φ_H), due to the self-organizing of Tp DLCs.

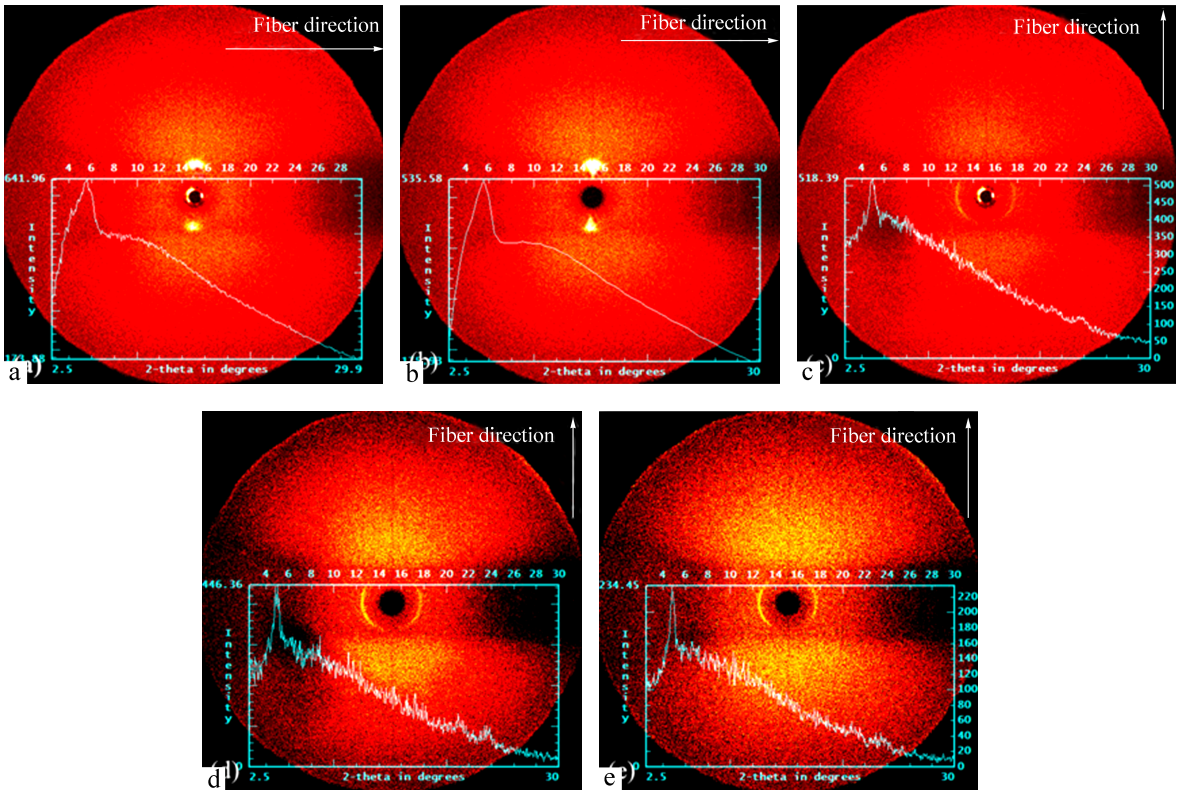


Fig. 10 2D WAXD pattern of PMTS (a), PMT2S (b), PMT3S (c), PMT4S (d) and PMT6S (e) at room temperature with the X-ray beam perpendicular to the fiber direction

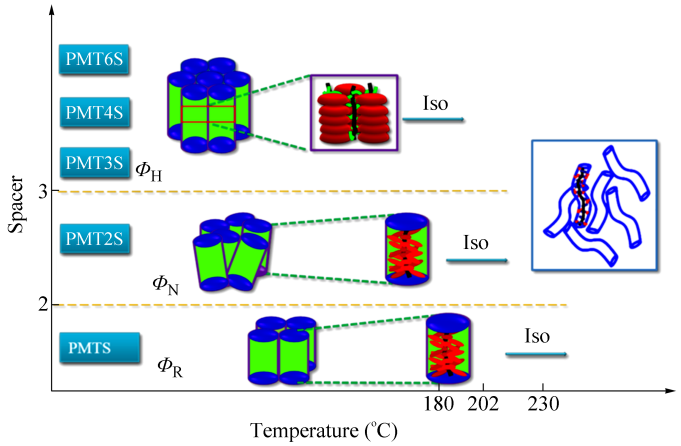


Fig. 11 Schematic drawing of the polymers

CONCLUSIONS

In summary, a series of SCLCPs containing Tp units in the side chains, with different lengths of spacers were successfully synthesized through conventional free radical polymerization. The phase behaviors were studies by DSC, POM, 1D and 2D WAXD. Polymers having no or short spacer form Φ_R phase (PMTS) or Φ_N phase (PMT2S), because the backbones and the Tp DLCs mesogenic groups cooperate together to construct cylinders as the building blocks.

In contrast, with increasing the length of flexible spacer ($n \geq 3$), which links fundamentally distinct LC building blocks, the phase behaviors of PMT*n*S (n = 3, 4, 6) vary tremendously and all the samples displayed symmetry Φ_H phase. It was considered that the polymer presented Φ_H phase of Tp discotic mesogens based on decoupling between the main chain and the Tp side chain. Compared with PMTS and PMT2S, the interaction between the main chain and the Tp is gradually weakened with the length of flexible spacer increasing, and ordered structures were developed by π-stacking of these Tp mesogens which tend to display their individual self-organizing properties. The formation mechanism of these different LC phases indicated that the "decoupling effect" or "coupling effect" depended on the length of spacer. Studies on the phase behaviors of these Tp DLCs polymers can provide new functional materials with stabilized and fine-tuning ordered structures, which will be useful for both fundamental research and real applications.

REFERENCES

1 Wu, X., Cao, H., Guo, R., Li, K., Wang, F., Gao, Y., Yao, W., Zhang, L., Chen, X. and Yang, H., Macromolecules, 2012, 45: 5556
2 Nobuhiro, K., Hitomi, M., Teppei, W., Mami, K. and Mizuho, K., Macromolecules, 2012, 45: 8547
3 Liu, X.Q., Wang, J., Yang, S. and Chen, E.Q., ACS Macro. Lett., 2014, 3: 834
4 Srividhya, D., Manjunathan, S., Nithyanandan, S., Balamurugan, S. and Senthil, S., Chinese J. Polym. Sci., 2009, 27(6): 761
5 Zheng, J.F., Liu, X., Chen, X.F., Ren, X.K., Yang, S. and Chen, E.Q., ACS. Macro. Lett., 2012, 1: 641
6 Nobuhiro, K., Hitomi, M., Teppei, W., Mami, K. and Mizuho, K., Macromolecules, 2012, 45: 8547
7 Wan, X., Tu, H., Liu, Y., Zhang, D., Chen, X., Zhang, H. and Zhou, Q., Chinese J. Polym. Sci., 2003, 21(1): 21
8 Yu, Z.Q., Jacky, W.Y.L., Zhu, C.Z., Chen, E.Q. and Tang, B.Z., Macromolecules, 2013, 46: 588
9 Liu, Y., Li, Y. and Xiong, H., ACS Macro. Lett., 2013, 2: 45
10 Prashant, D., Suk-kyun, A., Ludovic, G.M. and Rajeswari, M.K., Macromolecules, 2013, 46: 8245
11 Ni, B., Liao, J.Q., Chen, S. and Zhang, H.L., RSC Adv., 2015, 5: 9035
12 Deng, W., Brûlet, A., Albouy, P.A., Keller, P. and Li, M.H., Chinese J. Polym. Sci., 2012, 30: 258
13 Percec, V. and Tomazos, D., "Comprehensive polymer science", First Suppl., ed. Aggarwal, S.L. and Russo, S., Pergamon Press, Oxford, 1992, ch. 14
14 Sergeyev, S., Pisula, W. and Geerts, Y.H., Chem. Soc. Rev., 2007, 36: 1902
15 Pal, S.K. and Kumar, S., Liq. Cryst., 2008, 35: 381
16 Scherf, U., Gutacker, A. and Koenen, N., Acc. Chem. Res., 2008, 41: 1086
17 Chen, X., Chen, L., Yao, K. and Chen, Y., ACS Appl. Mater. Interfaces, 2013, 5: 8321
18 Emiliano, T., Rubeń, C., Gerardo, S.E., Ceśar, L.F., Josu, O., Silverio, C. and Pablo, E., Inorg. Chem., 2014, 53: 3449
19 Julien, I., RaphaeÏ, M., Laurent, D., Freḑeŕic, C., Harald, B., Yoann, O., Jeŕom̂e, C., David, B., Gabriele, D.A., Otello, M.R., Luca, M. and Claudio, Z., J. Am. Chem. Soc., 2014, 136: 2911
20 Danli, Z., Ibtissam, T.D., Yiming, X., Farid, K., Navaphun, K., Martin, B., Daniel, G., Benoît, H., Bertrand, D., Dimitri, A.I., Emmanuelle, L., David, K., Fabrice, M. and Andre-́Jean, A., Macromolecules, 2014, 47: 1715
21 Chandrasekhar, S., Sadashiva, B.K. and Suresh, K.A., Pramana, 1977, 9: 471
22 Kumar, S., Liq. Cryst., 2004, 31: 1037

23 Kumar, S., Liq. Cryst., 2005, 32: 1089
24 Karoda, H., Goto, H., Akagi, K. and Kawaguchi, A., Macromolecules, 2002, 35: 1307
25 Ting, C.H., Chen, J.T. and Hsu, C.S., Macromolecules, 2002, 35: 1180
26 Kong, X.F., He, Z.Q., Gopee, H. and Cammidge, A.N., Liq. Cryst., 2011, 38: 943
27 Ibtissam, T.D., Nekelson, F., Heinrich, B., Donnio, B., Guillon, D., Kreher, D., Mathevet, F. and Attias, A.J., Chem. Mater., 2011, 23: 4653
28 Hüser, B. and Spiess, H.W., Macromol. Rapid Commun., 1988, 9: 337
29 Hüser, B., Pakula, T. and Spiess, H.W., Macromolecules, 1989, 22: 1960
30 Ringsdorf, H., Wuštefeld, R., Zerta, E., Ebert, M. and Wendorff, J.H., Angew. Chem., Int. Ed., 1989, 28: 914
31 Werth, M. and Spiess, H.W., Macromol. Rapid Commun., 1993, 14: 329
32 Stewart, D., Mchattie, S.G. and Imrie, C.T., J. Mater. Chem., 1998, 8: 47
33 Boden, N., Bushby, R.J. and Lu, Z.B., Liq. Cryst., 1998, 25: 47
34 Imrie, C.T., Inkster, R.T., Lu, Z. and Ingram, M.D., Mol. Cryst. Liq. Cryst., 2004, 408: 33
35 Xing, C.M., Lam, J.W.Y., Zhao, K.Q. and Tang, B.Z., J. Polym. Sci., Part A: Polym. Chem., 2008, 46: 2960
36 Yu, Z.Q., Jacky, W.Y.L., Zhao, K., Zhu, C.Z., Yang, S., Lin, J.S., Li, B.S., Liu, J.H., Chen, E.Q. and Tang, B.Z., Polym. Chem., 2013, 4: 996
37 Zhu, Y.F., Guan, X.L., Shen, Z.H., Fan, X.H. and Zhou, Q.F., Macromolecules, 2012, 45: 3346
38 Zhu, Y.F., Tian, H.J., Wu, H.W., Hao, D.Z., Zhou, Y., Shen, Z.H., Zou, D.C., Sun, P.C., Fan, X.H. and Zhou, Q.F., J. Polym. Sci., Part A: Polym. Chem., 2014, 52: 295
39 Finkelmann, H., Michael, H., Michael, P. and Ringsdorf, H., Makromol. Chem., 1978, 179: 2541
40 Finkelmann, H., Ringsdorf, H. and Wendorff, J.H., Makromol. Chem., 1978, 179: 273
41 Gemmell, P.A., Gray, G.W., Lacey, D., Alimoglu, A.K. and Ledwith, A., Polymer, 1985, 26: 615
42 Yamaki, S., Nakagawa, M., Morino, S. and Ichimura, K., Macromol. Chem. Phys., 2001, 202: 354
43 Percec, V., Aqad, E., Eterca, P.M., Rudick, J.G., Lemon, L., Ronda, J.C., De, B.B., Heiney, P.A. and Meije, E.W., J. Am. Chem. Soc., 2006, 128: 16365
44 Percec, V., Rudick, J.G., Peterca, M., Aqad, E., Imam, M.R. and Heiney, P.A., J .Polym. Sci., Part A: Polym. Chem., 2007, 45: 4974
45 Percec, V., Rudick, J.G., Peterca, M. and Heiney, P.A., J. Am. Chem. Soc., 2008, 130: 7503
46 Craig, A.A. and Imrie, C.T., J. Mater. Chem., 1994, 4: 1705
47 Craig, A.A. and Imrie, C.T., Macromolecules, 1995, 28: 3617
48 Ban, J.F., Chen, S., Li, C., Wang, X.Z. and Zhang, H.L., Polym. Chem., 2014, 5: 6558
49 Ban, J.F., Chen, S. and Zhang, H.L., RSC Adv., 2014, 4: 54158
50 David, S., Gillian, S.M. and Corrie, T.I., J. Mater. Chem., 1998, 8(1): 47
51 Percec, V., Bera, T.K., Glodde, M., Fu, Q., Balagurusamy, V.S.K. and Heiney, P.A., Chem. Eur. J., 2003, 9: 921
52 Percec, V., Imam, M.R., Peterca, M. and Leowanawat, P., J. Am. Chem. Soc., 2012, 134: 4408
53 Al-Lawati, Z.H., Bushby, R.J. and Evans, S.D., J. Phys. Chem. C., 2013, 117: 7533
54 Chen, X.F., Shen, Z.H., Wan, X.H., Fan, X.H., Chen, E.Q., Ma, Y.G. and Zhou, Q.F., Chem. Soc. Rev., 2010, 39: 3072
55 Xie, H.L., Wang, S.J., Zhong, G.Q., Liu, Y.X., Zhang, H.L. and Chen, E.Q., Macromolecules, 2011, 44: 7600
56 Paraschiv, I., de-Lange, K., Giesbers, M., van-Lagen, B., Grozema, F.C., Abellon, R.D., Siebbeles, L.D.A., Sudholter, E.J.R., Zuilhof, H. and Marcelis, A.T.M., J. Mater. Chem., 2008, 18: 5475